scientific reports

Check for updates

OPEN

Genome-wide analysis uncovers tomato leaf lncRNAs transcriptionally active upon *Pseudomonas syringae* pv. *tomato* challenge

Hernan G. Rosli[1]✉, Emilia Sirvent[1], Florencia N. Bekier[1], Romina N. Ramos[1,2] & Marina A. Pombo[1]✉

Plants rely on (in)direct detection of bacterial pathogens through plasma membrane-localized and intracellular receptor proteins. Surface pattern-recognition receptors (PRRs) participate in the detection of microbe-associated molecular patterns (MAMPs) and are required for the activation of pattern-triggered immunity (PTI). Pathogenic bacteria, such as *Pseudomonas syringae* pv. *tomato* (*Pst*) deploys ~ 30 effector proteins into the plant cell that contribute to pathogenicity. Resistant plants are capable of detecting the presence or activity of effectors and mount another response termed effector-triggered immunity (ETI). In order to investigate the involvement of tomato's long non-coding RNAs (lncRNAs) in the immune response against *Pst*, we used RNA-seq data to predict and characterize those that are transcriptionally active in leaves challenged with a large set of treatments. Our prediction strategy was validated by sequence comparison with tomato lncRNAs described in previous works and by an alternative approach (RT-qPCR). Early PTI (30 min), late PTI (6 h) and ETI (6 h) differentially expressed (DE) lncRNAs were identified and used to perform a co-expression analysis including neighboring (± 100 kb) DE protein-coding genes. Some of the described networks could represent key regulatory mechanisms of photosynthesis, PRR abundance at the cell surface and mitigation of oxidative stress, associated to tomato-*Pst* pathosystem.

Plants are under the attack of different kind of pathogens and this provokes economical losses all around the world[1]. However, to defend themselves they possess a diversified innate immune system that consists in membrane and cytoplasmic receptors that are able to detect different pathogen features[2,3]. Pattern recognition receptors (PRRs) are on the surface of the plant cell and can recognize microbe-associated molecular patterns (MAMPs), activating an immune response named pattern-triggered immunity (PTI)[4]. This response includes production of reactive oxygen species (ROS), callose deposition into the apoplast, activation of MAP kinase cascades, increase of intracellular calcium concentration and transcriptional reprograming[5–8].

Pathogenic bacteria such as *Pseudomonas syringae* pv. *tomato* (*Pst*) can introduce inside the plant cell cytoplasm effector proteins that are able to undermine PTI and also interfere with cellular processes for the promotion of their own growth, multiplication in the apoplast and virulence[9,10]. However, some plants have acquired resistance proteins (R proteins), most of them nucleotide-binding leucine-rich repeat proteins (NLRs) that can directly or indirectly detect some of these effectors. After this detection, they activate another immune response called effector-triggered immunity (ETI) or more recently named NLR-triggered immunity (NTI)[11,12]. ETI activation also includes ROS production, MAPK signaling, electrolyte leakage into the apoplast and transcriptional reprograming[13,14], but it is characterized for the development of a hypersensitive response (HR) that culminates in programmed cell death (PCD)[15]. In addition, some effectors are involved in the suppression of this immune response[16].

Tomato (*Solanum lycopersicum*) is an economically important crop that is produced all around the world. The interaction between tomato and *Pseudomonas syringae* pv. *tomato* (*Pst*), the causal agent of tomato speck disease,

[1]Instituto de Fisiología Vegetal, INFIVE, Universidad Nacional de La Plata, CONICET, La Plata, Buenos Aires, Argentina. [2]Facultad de Ciencias Exactas, Universidad Nacional de La Plata, La Plata, Buenos Aires, Argentina. ✉email: hrosli@agro.unlp.edu.ar; mpombo@agro.unlp.edu.ar

is used for the study of the molecular mechanisms implicated in bacterial pathogenesis and plant defenses[17,18]. Most of the transcriptional changes that occur upon *Pst*-mediated PTI activation in tomato are due to the perception of flagellin, the main component of bacterial flagella[7]. Tomato recognizes two epitopes of flagellin, flg22 and flgII-28, which are detected by the receptors FLS2 and FLS3, respectively[19–21].

Pst DC3000 can introduce more than 30 effectors into the plant cell[22]. Two of them, AvrPto and AvrPtoB, interfere with PTI signaling right after MAMP detection[7,23]. However, resistant tomatoes can detect these two effectors through a protein kinase Pto that jointly with the NLR Prf, activate a strong ETI[18,24–26].

The development of high sensitive sequencing technologies such as RNA-seq has allowed the identification of new transcripts, much of them not derived from annotated protein coding-genes[27]. For some time they were considered as "junk DNA", but then more and more studies supported the idea that some of these non-coding RNAs (ncRNAs) possess important regulatory functions in different cellular processes[27]. Long non-coding RNAs (lncRNAs) are a subset of ncRNAs with an established size of 200 bp or more[28]. They are transcribed from diverse regions in the genome and according to this are classified in intergenic, intronic, overlapping with coding genes, sense and antisense, among others[29].

Depending on their location inside the cell, they are believed to modulate different processes. Nuclear lncRNAs can regulate transcription of protein coding genes through chromatin modification, recruitment of transcription inhibitors or enhancers, enabling the proximity between enhancer sequences and transcription start sites and modulate alternative splicing by interacting with different splicing factors[30]. In the case of the cytoplasmic lncRNAs, they have been implicated in messenger RNA (mRNA) stability for example, acting as "sponges" of micro RNA (miRNA) avoiding their target mRNA degradation or producing small interference RNAs (siRNA) after being cut by a miRNA, that can subsequently lead to the degradation of other mRNAs[31]. Some lncRNAs interact with ribosomal proteins and therefore regulate mRNA translation to protein[32,33].

Although less studied than in humans, lncRNAs are rising as important players in plants too[32,34,35]. In this sense, they have been involved in the regulation of different biological processes such as phosphorous nutrition deficiency[36], sexual reproduction[37], vernalization and floral timing[38,39], abiotic[40] and biotic stresses[41,42].

Related with plant–pathogen interactions, previously and using microarrays, lncRNAs with higher expression after plant treatment with elf 18 (MAMP derived from the elongation factor Tu) were identified in Arabidopsis[41]. Then, ELF18-INDUCED LONG-NONCODING RNA1 (ELENA1) was functionally characterized as an intergenic lncRNA with active transcription after elf18 and flg22 perception. Plants with reduced levels of ELENA1 were more susceptible to *Pst* DC3000, while plants over-expressing ELENA1 developed an opposite phenotype, showing that this lncRNA acts as a positive regulator of plant defenses against this pathogen[42].

Particularly in tomato, several lncRNAs were identified as expressed during fruit ripening[43,44]. In addition, tomato lncRNAs have been described as associated to interactions with virus[45,46], viroid[47] and the oomycetes *Phytophthora infestans*[48–51]. Until now, there are no reports of lncRNA with induced expression in the tomato-*Pst* pathosystem.

In the present work, we re-analyzed previously published RNA-seq data from tomato, derived from a large set of treatments/conditions[7,52,53]. Through this approach we were able to identify and characterize lncRNAs that are expressed in tomato leaves and determine those differentially expressed in early PTI (30 min), late PTI (6 h) and ETI at 6 h. By means of transcriptional co-regulation analysis including lncRNAs and protein-coding genes, a group of relevant networks were identified. Some of these could be part of the mechanisms behind the regulation of processes such as of photosynthesis, PRR abundance at the plasma membrane and oxidative stress response, upon *Pst* challenge in tomato plants.

Results

Tomato lncRNA identification. For our analysis we used a set of previously generated RNAseq data that includes 11 different treatments/controls (flg22, flgII-28 or different Pseudomonas spp. strains), each with three biological replicates (Table S1). The selection of these conditions was motivated by the fact that through certain comparisons we could capture lncRNA transcriptomic changes associated to early and late PTI (30 min and 6 h), ETI and the effect of two *Pst* DC3000 effectors (AvrPto and AvrPtoB) in suppressing PTI. We identified 22,595 novel tomato transcripts which were used as input for a pipeline (see "Materials and methods") that allowed the prediction of 2609 putative lncRNAs transcriptionally active in tomato leaves under these conditions (Table S2). We investigated the degree of overlap between our predicted lncRNAs for the tomato-*Pst* pathosystem and those available from previous works using tomato under different conditions. Already identified tomato leaf lncRNAs included those detected upon challenge with Tomato yellow curl leaf virus (TYCLV)[45,46,54] or *Phytophthora infestans*[48,55], those available for tomato in CANTATA database[56] and four predicted tomato *TRANS-ACTING SIRNA3* (*TAS3*) transcripts[57]. Performing a local blastn[58] using our predicted lncRNAs as query and those derived from previous works as database, we found that 1247 (47.7%) of query sequences had at least one hit, with an overall average identity of 97.6% (Table S3). The remaining transcripts without match to those previously identified could account for lncRNAs that are transcriptionally active upon elicitation of tomato immune response by *Pseudomonas* spp. or MAMPs challenges and time-points used in this work (30 min and 6 h). It is worth mentioning that we cannot assume these "novel" lncRNAs we identified are specific of the bacterial pathosystem under study. We continued our analysis with all the lncRNAs predicted in this work, regardless of their being previously identified.

Analysis of the number of isoforms, indicated that the large majority of lncRNA genes (2141; 82%) encoded for a single isoform (Fig. S1). We defined a lncRNA as "expressed" if it had ≥ 3 FPKM (fragments per kilobase per million mapped reads) in at least one of the 11 conditions analyzed. From the 2609 lncRNAs we predicted with our pipeline, only these "expressed" lncRNAs (2048; Table S4) were considered from this point on, unless stated otherwise.

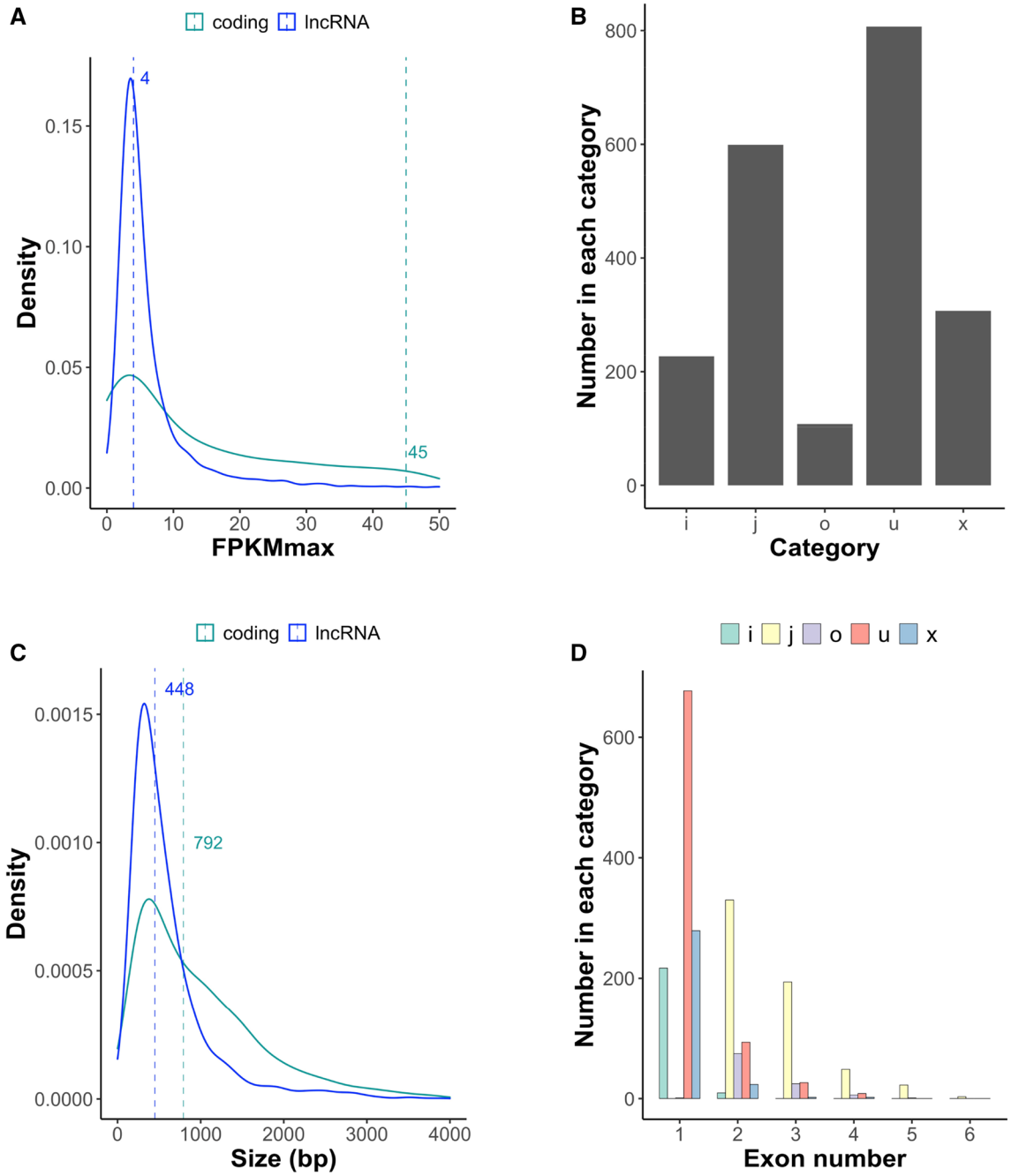

Figure 1. Global characterization of tomato lncRNAs and comparison with protein-coding genes. (**A**) Transcript abundance distribution considering maximum FPKM (FPKMmax) value from all samples and excluding those with FPKMmax = 0. The position of median value is indicated for each distribution. (**B**) Expressed lncRNAs (FPKM ≥ 3 in at least one sample) in categories based on their relationship to annotated tomato transcripts[59]. (**C**) Transcript size distribution of expressed lncRNAs and tomato protein-coding genes. The position of median value is indicated for each distribution. (**D**) Gene structure of expressed lncRNAs falling in the different categories based on their relationship to annotated tomato transcripts.

Global characterization of tomato lncRNAs. We analyzed the distribution of expression levels of protein-coding and lncRNA transcripts, excluding those with rounded average FPKM = 0 (Fig. 1A). LncRNAs' FPKM median value was nearly tenfold smaller than that for protein-coding tomato genes, indicating that lncRNAs have overall lower expression levels as previously shown for Arabidopsis [34]. From the 2048 expressed lncRNAs identified the most abundant categories, in terms of their relationship to annotated transcripts[59], were *u* (unknown, intergenic transcript) and *j* (potentially novel isoform with at least one splice junction shared with reference transcript), while category *o* (generic exonic overlap with a reference transcript) was the least represented (Fig. 1B). We investigated how protein-coding and lncRNA transcript size distribution compared.

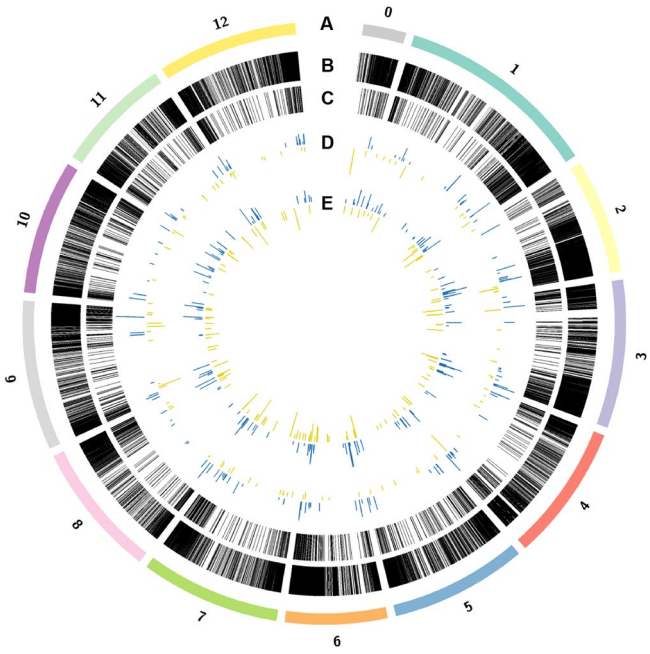

Figure 2. Genomic distribution of lncRNAs and protein-coding genes. (**A**) tomato chromosomes, (**B**) protein-coding genes, (**C**) lncRNAs, (**D**) DELs mock_flgII-28_6h vs flgII-28_6h (PTI-flgII28, 6 h), (**E**) DELs for *Pst* DC3000 Δ*fliC*Δ*avrPto*Δ*avrPtoB* vs *Pst* DC3000 Δ*fliC* in PtoR background (ETI, 6 h). Induced and suppressed transcripts are indicated with blue and yellow lines, respectively. The length of these lines is proportional to the transcript fold-change in each comparison.

Protein-coding transcripts' distribution shifted towards larger sizes with a median value that almost doubled the observed for lncRNAs (Fig. 1C).

To further characterize the identified tomato lncRNAs we studied the number of exons for transcripts in each category (Fig. 1D). For categories *i*, *u* and *x* most transcripts contained a single exon while for those in categories *j* and *o*, 2-exon transcripts were most abundant. Overall, 1-exon transcripts accounted for 1174 lncRNAs (57% of all expressed lncRNAs).

The distribution of lncRNAs in tomato chromosomes did not differ from the one observed for protein-coding genes (Fig. S2), ranging from 7 to 12% for chromosomes 1–12. We then analyzed the position within each chromosome where protein-coding (Fig. 2, lane B) and lncRNAs (Fig. 2, lane C) reside. Both types of transcripts are encoded mainly at the beginning and ending of each chromosome. These findings indicate there are no obvious lncRNA-specific hot spots in the genome and that these are encoded in the same regions as protein-coding genes.

LncRNAs' expression changes associated to tomato immunity. Setting a cut-off of q-value < 0.05 and |log2 fold-change| ≥ 1, we established differentially expressed lncRNAs (DELs) for the comparisons of interest (Table S4 and Fig. 3). Early flg22-associated PTI induction lead to a small set of DELs (26 up- and 8 down-regulated). Contrastingly, for flgII-28 challenge at 6 h time-point the number of DELs was clearly larger, suggesting a stronger immune response at the transcriptional level (118 up- and 82 down-regulated). Leaf infiltration with the strong PTI inducer, *Pseudomonas fluorescens* 55, lead to a number of DELs that were fewer than those identified for flgII-28. This finding is in agreement with the data that derives from the same treatments, but for protein-coding transcripts differentially expressed genes (DEGs)[7]. We compared DC3000 vs DC3000 Δ*avrPto*Δ*avrPtoB* in RG-*prf3* susceptible plants. With this comparison, which accounts for the effect of AvrPto and AvrPtoB effectors at the transcriptional level, we observed that up-regulation of lncRNAs prevailed over down-regulation. This same trend had been previously found for protein-coding genes[7].

A group of transcripts of particular interest are those induced by flgII-28 treatment and suppressed by AvrPto and/or AvrPtoB effectors (DC3000 < DC3000 Δ*avrPto*Δ*avrPtoB* in RG-*prf3* susceptible plants). This group of transcripts were previously termed FIRE (flagellin-induced, repressed by effectors) which allowed the identification of a tomato wall associated kinase, SlWak1, that participates in the immunity against *Pst*[7,60]. We were able to identify a set of 20 FIRE lncRNAs (Table S4 and Fig. 3) which accounts for ~ 57% of those suppressed by AvrPto and/or AvrPtoB in RG-*prf3*. In contrast, in the case of protein-coding genes, this percentage is considerably higher (~ 91%)[7].

AvrPto- and/or AvrPtoB-induced ETI (DC3000 Δ*fliC*Δ*avrPto*Δ*avrPtoB* vs. DC3000 Δ*fliC* in PtoR background) lead to the highest numbers of DELs of all treatments analyzed, both up- and down-regulated, while flagellin-associated PTI was associated to a milder transcriptional response (Table S4 and Fig. 3). A similar behavior was observed for protein-coding genes under the same challenges[52].

In order to globally analyze lncRNA transcriptional changes, we performed separate clustering analysis data deriving from RG-*prf3* and RG-PtoR tomato lines' challenges. Treatments in RG-*prf3* plants formed three clear

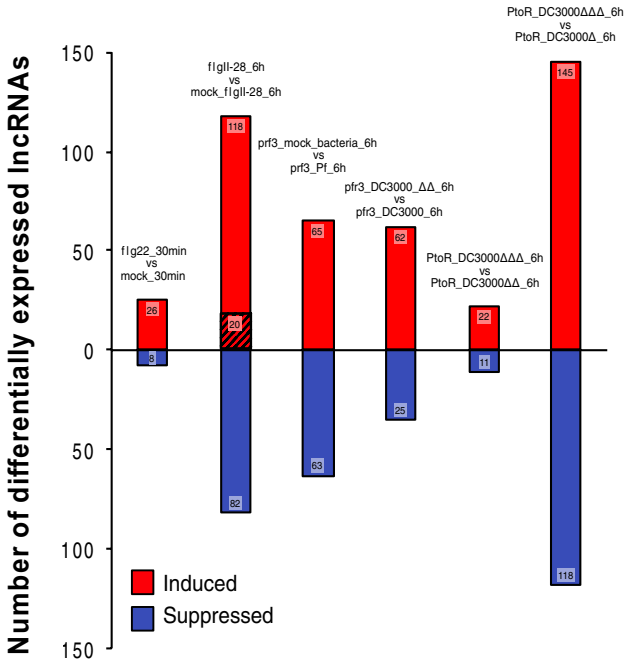

Figure 3. Differentially expressed lncRNAs (DELs). For each comparison, number of induced and suppressed DELs (q-value < 0.05 and |log2 fold-change| ≥ 1) is shown inside the graph bar. Striped pattern in flgII-28_6h vs mock_flgII-28_6h represents number of FIRE DELs. prf3_Pf_6h (*Pseudomonas fluorescens* in RG-*prf3* background); prf3_DC3000_6h (*Pst* DC3000 in RG-*prf3* background); prf3_DC3000ΔΔ_6h (*Pst* DC3000 Δ*avrPto*Δ*avrPtoB* in RG-*prf3* background); PtoR_DC3000Δ_6h (*Pst* DC3000 Δ*fliC* in RG-PtoR background); PtoR_DC3000ΔΔ_6h (*Pst* DC3000 Δ*avrPto*Δ*avrPtoB* in RG-PtoR background); PtoR_DC3000ΔΔΔ_6h (*Pst* DC3000 Δ*fliC*Δ*avrPto*Δ*avrPtoB* in RG-PtoR background).

clusters that can be categorized as 30 min time-points, PTI-inducing treatments and mock treatments; these last two, at 6 hai (Fig. 4A). It is worth mentioning that grouping along with mock treatments, was DC3000 challenge in RG-*prf3* plants, which can be associated to the effect of AvrPto and/or AvrPtoB in suppressing PTI response at the transcriptional level of protein coding genes[7]. Distinct transcript clusters included: 1, PTI induced at 6 hai (including some FIRE lncRNAs); 2, early flg22 induced; 3, PTI suppressed at 6 hai (Fig. 4A). Within cluster 1, some transcripts following FIRE transcriptional changes can be visualized. In the case of treatments in RG-PtoR background clustering (PtoR_DC3000ΔΔΔ grouping with PtoR_DC3000ΔΔ) was in agreement with having found a larger number of DELs for the comparison PtoR_DC3000ΔΔΔ vs PtoR_DC3000Δ, than in PtoR_DC3000ΔΔΔ vs PtoR_DC3000ΔΔ (Figs. 3 and 4B). Transcript clustering allowed the identification of groups of lncRNAs associated to strong PTI/ETI suppression/induction (Fig. 4B).

Evaluation of lncRNAs' expression by RT-qPCR. For this purpose we selected several lncRNAs: two induced by *P. fluorescens* 55 treatment (PTI, prf3_mock_bacteria_6h vs prf3_Pf_6h), two induced by ETI (DC3000 Δ*fliC*Δ*avrPto*Δ*avrPtoB* vs. DC3000 Δ*fliC* in PtoR background) and one induced by both immune responses. We challenged an independent set of RG-PtoR plants to induce PTI (mock vs *P. fluorescens* 55) and ETI (DC3000 Δ*avrPto*Δ*avrPtoB* vs DC3000) and sampled at the same time-point as the one used for the RNA-seq experiment (6 hai). For all selected lncRNAs we were able to detect their corresponding transcripts and to confirm their transcriptional changes upon PTI and/or ETI activation (Fig. 5).

Gene ontology (GO) term analysis and co-expression networks. Transcriptional co-regulation of lncRNAs and neighboring protein-coding genes could help identify networks that are modulated by lncRNAs. Such regulation represents one of lncRNAs' mechanisms to control gene expression (cis-action)[31]. In our case we were interested in identifying lncRNAs that modulate key protein-coding genes involved in tomato defense response against *Pst*. For up-regulated DELs identified in the comparisons mock_flgII-28_6h vs flgII-28_6h (PTI-flgII-28) and DC3000 Δ*fliC*Δ*avrPto*Δ*avrPtoB* vs. DC3000 Δ*fliC* in PtoR background (ETI-AvrPto/AvrPtoB), we identified those neighboring (within a 100 Kb genome region[48,61–63]) protein-coding genes whose transcriptional behavior was the same (up-regulated, positive co-regulation) or opposite (down-regulated, negative co-regulation) for these same comparisons, using |log2 fold-change| ≥ 1 and q-value < 0.05 as cut-offs. This set of genes was termed neighboring protein-coding co-regulated genes (NCG). Though gene ontology (GO) term analysis of PTI-flgII-28 induced DELs' NCG with positive co-regulation (121 coding genes) resulted in no enrichment, "kinase activity" was one terms with the lowest p-value and was assigned to 10 NCGs (Table S5). Negatively co-regulated NCGs (82 total coding genes) were enriched in the term "photosynthesis" (Table S5),

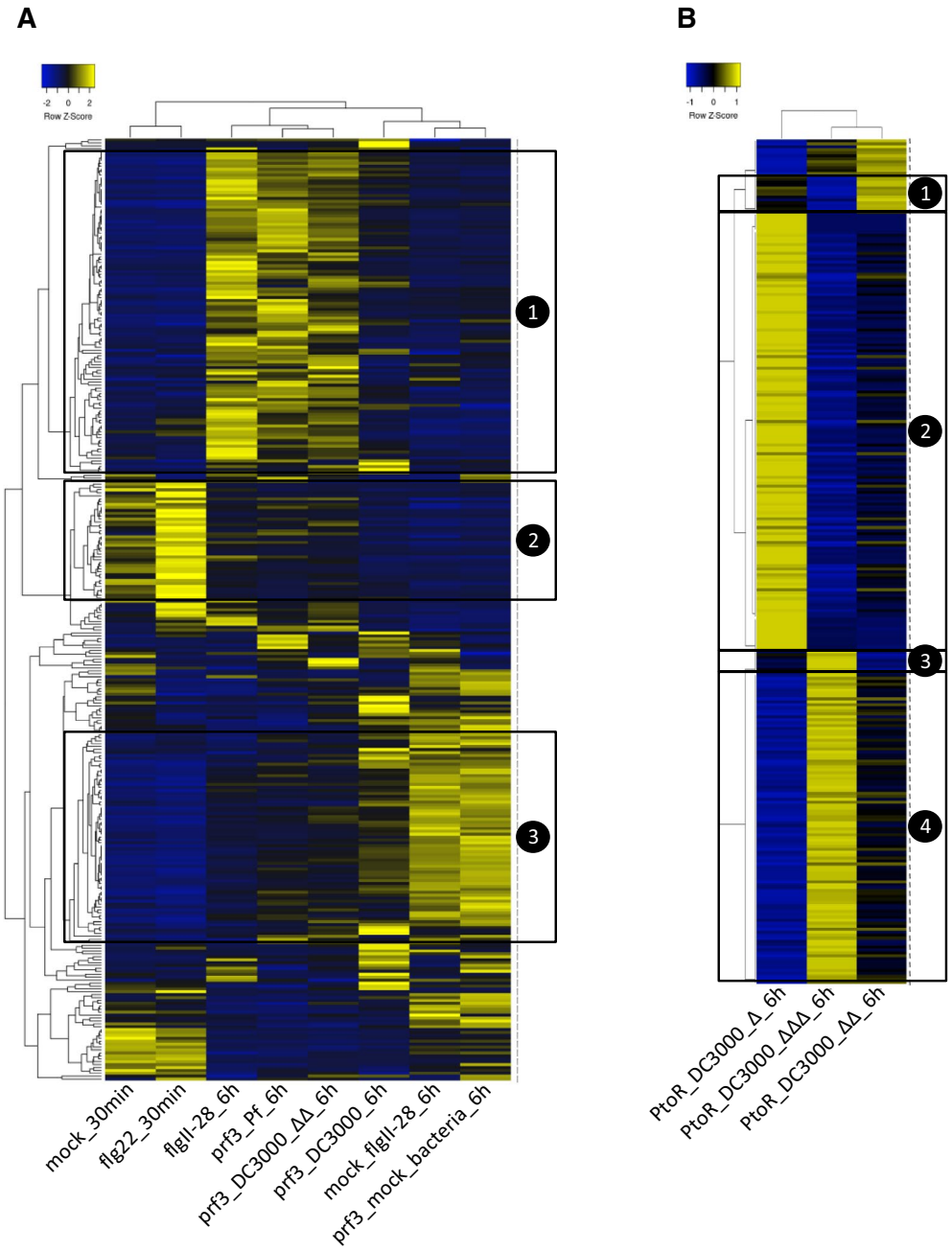

Figure 4. Clustering analysis based on lncRNAs and treatments. LncRNAs included in each cluster had at least one comparison of interest, indicated in Fig. 3, with q-value < 0.05. (**A**) Cluster for treatments in RG-*prf3* plants with the following groups highlighted: 1, induced by PTI at 6 h; 2, induced by flg22 at 30 min; 3, suppressed by PTI at 6 h. (**B**) Cluster for treatments in RG-PtoR plants with the following groups highlighted: 1, strong PTI induction; 2 strong ETI induction; 3, strong PTI suppression; 4, strong ETI suppression. *Pst* DC3000 mutants' nomenclature is described in Fig. 3 legend.

indicating that the corresponding DELs could be controlling transcript abundance of these NCGs and consequently leading to a suppression of the photosynthesis-related genes during PTI activation.

The analysis of the 221 NCGs with positive co-regulation with ETI up-regulated DELs, revealed that "transcription factor activity, sequence-specific DNA binding" was one of the terms with lowest p-value (Table S6). Again for negatively co-regulated NCGs we found an enrichment of "photosynthesis" term. Indicating that lncRNAs may participate in the negative modulation of photosynthesis-related genes during both PTI and ETI induction.

To further understand the relationships between lncRNAs and their co-regulated coding genes we performed a network analysis including PTI-flgII-28- and ETI-AvrPto/AvrPtoB-induced NCGs. Complete networks can be found in Figs. S3–S6, while selected ones are shown in Fig. 6. We could identify networks that are exclusive

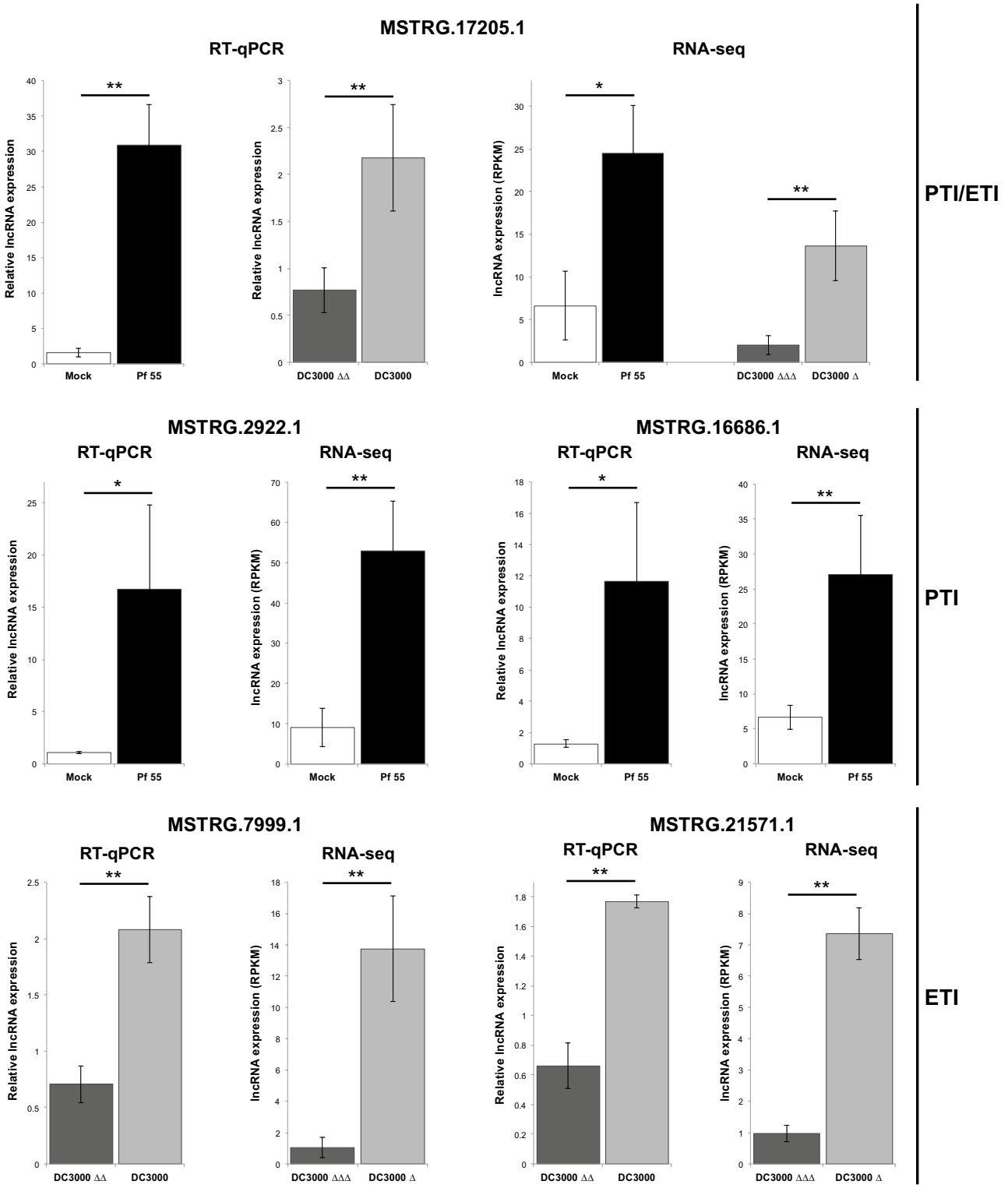

Figure 5. Expression analysis of selected DELs by RT-qPCR. Analyzed transcripts include PTI-, ETI- and PTI/ETI-responsive lncRNAs. Bars represent the median of 3 biological replicates and 3 technical replicates each, with their corresponding standard deviation. For RT-qPCR results, * or ** represent statistical differences using Student's *t*-test 0.05 and 0.01, respectively. For RNA-seq results, * represents q-value < 0.05 and ≥ twofold change, while ** q-value < 0.01 and |log2 fold-change| ≥ 1. Pf 55 (*Pseudomonas fluorescens* 55); PtoR_DC3000Δ_6h (*Pst* DC3000 Δ*fliC* in RG-PtoR background); PtoR_DC3000ΔΔΔ_6h (*Pst* DC3000 Δ*fliC*Δ*avrPto*Δ*avrPtoB* in RG-PtoR background).

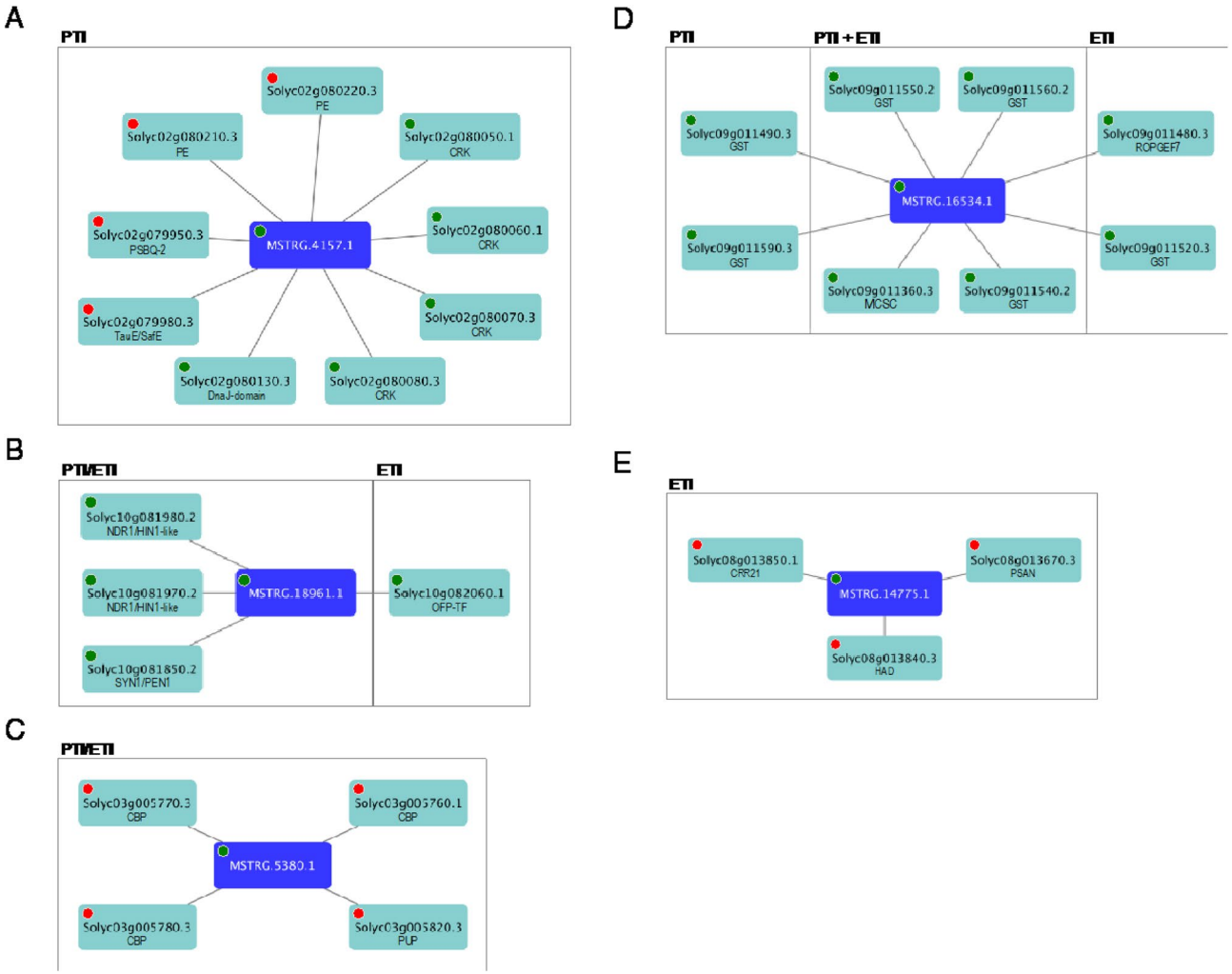

Figure 6. Selected DELs—neighboring protein-coding co-regulated genes (NCG) networks. For DELs found in the comparisons prf3_mock_flgII28_6h vs prf3_flgII-28_6h (PTI) and DC3000 Δ*fliC*Δ*avrPto*Δ*avrPtoB* vs DC3000 Δ*fliC* at 6 h in PtoR plants (ETI) their NCG were identified and used to generate the networks. (**A**) PSBQ-2 (Photosystem II subunit Q-2); TauE/SafE (Sulfite exporter TauE/SafE); PE (Pectinesterase); CRK (Cystein-rich receptor-like kinase); DnaJ-domain (Chaperone DnaJ-domain superfamily). (**B**) SYN/PEN1 (Syntaxin 1/Penetration 1); NDR1/HIN1-like (Arabidopsis non-race specific disease resistance gene 1/Harpin-induced gene 1); OFP-TF (Ovate family protein (OFP) transcription factor). (**C**) CBP (Chlorophyll a/b-binding protein); PUP (Purine permease). (**D**) GST (Glutathione S-transferase); ROPGEF7 (ROP (Rho of plants) guanine nucleotide exchange factor 7); MCSC (Mitochondrial substrate carrier family protein). (**E**) CRR21 (Chlororespiratory reduction 21); HAD (Haloacid dehalogenase-like hydrolase); PSAN (Photosystem I reaction center subunit PSI-N). Red and green circles indicate suppression or induction in the comparisons evaluated, respectively.

of PTI-flgII-28 (Fig. 6A) or ETI-AvrPto/AvrPtoB (Fig. 6E), but also common ones (Fig. 6B–D). MSTRG.4157.1, a category x and PTI-flgII-28-induced lncRNA, was member of one of the largest networks found. In this case NCGs included transcripts up- and down-regulated by PTI-flgII-28 activation. Four up-regulated NCGs encode for cystein-rich receptor-like kinases and one for a chaperone, while down-regulated NCGs included transcripts coding for cell wall degrading enzymes, a photosystem II subunit and a sulfite transporter (Fig. 6A).

The network of MSTG.18961.1 (Fig. 6B), an intronic lncRNA of Solyc10g081980.2, contained Solyc10g081850.2 whose closest protein in *Arabidopsis thaliana* is AT3G11820 (Penetration 1, PEN1) that has been recently proposed to have role in the accumulation of the receptor FLS2 at the plasma membrane[64]. Two Arabidopsis non-race specific disease resistance gene 1/Harpin-induced gene 1 (NDR1/HIN1)-like transcripts also belong to this network. Particularly interesting is Solyc10g081980.1 whose closest protein in A. thaliana is AT5G06320 (NDR1/HIN1-like 3, NHL3), a membrane-localized protein that when overexpressed leads to plants with increased resistance to pathogenic *Pst* DC3000[65].

Three PTI-flgII-28- and ETI-AvrPto/AvrPtoB-suppressed NCGs coding for chlorophyll a/b-binding proteins (CBP) form a network with MSTRG.5380.1, a DEL induced by these same immune responses (Fig. 6C). In this network we also identified a transcript encoding for a purine permease. Another lncRNA, but only induced by

ETI-AvrPto/AvrPtoB (Fig. 6E), shares a network with a transcript coding for CRR21 (Chlororespiratory reduction 21) which plays a role in chloroplast RNA editing of a subunit of the NAD(P)H complex, which is key for its function[66]. In addition, a transcript coding for PSAN (Photosystem I reaction center subunit PSI-N) was found to be part of this network. These lncRNAs could negatively impact the abundance of transcripts coding for key photosynthesis-related proteins.

Six transcripts coding for glutathione S-transferases (GST) that are induced by PTI-flgII-28- and/or ETI-AvrPto/AvrPtoB, belong to the network of MSTRG.16534.1, an intergenic lncRNA that may modulate these coding genes' transcript abundance (Fig. 6D). GSTs have been shown to participate in plant immunity against different types of pathogens[67].

Discussion

Taking advantage of a large set of RNA-seq data we were able to identify lncRNAs transcriptionally active in tomato leaves challenged with MAMPs and bacterial strains. Input RNA-seq data for prediction of novel transcripts represented 25× coverage of tomato genome and a stringent pipeline was used for lncRNA identification. The reliability of our approach was confirmed by comparing our set of lncRNAs with others described for tomato in previous publications and by analyzing gene expression by another methodology (RT-qPCR) the predicted transcriptional changes associated to different bacterial challenges.

Differential gene expression analysis of lncRNAs revealed that challenges with fewest and largest number of up-/down-regulated transcripts were mostly in agreement with what was observed for protein-coding genes[7,52]. This analysis allowed the identification of FIRE lncRNAs, which represent a promising set of candidates for studying their involvement in tomato immunity against *Pst*.

Effectors AvrPto and AvrPtoB have the capacity to suppress early recognition stages of PTI[68]. In agreement with this most of the genes suppressed by these effectors (DC3000 < DC3000 Δ*avrPto*Δ*avrPtoB* in RG-*prf3* plants) should also be induced by PTI (mock < flgII-28). That is the case for protein-coding genes, with a 91% of genes suppressed by AvrPto/AvrPtoB that are also induced by flgII-28[7]. This percentage is clearly lower (57%) for the case of lncRNAs analyzed in this work using the same exact challenges. This means that there is a larger proportion of lncRNAs that are suppressed by these effectors that are not modulated by PTI activation. This may be evidence of virulence exerted by AvrPto and AvrPtoB through manipulation of key lncRNAs' abundance, independently of their effect on PTI suppression.

To identify putative lncRNAs that may participate in plant immunity activation by modulating transcript abundance of neighboring protein-coding genes[30], we performed a network analysis that included PTI-flgII-28- and ETI-AvrPto/AvrPtoB-induced NCGs. This analysis revealed several interesting groups of transcripts whose abundance could be modulated by lncRNAs. Nuclear encoded chloroplast-targeted genes (NECGs) have been shown to be down-regulated upon activation of PTI, ETI or challenge with a pathogenic bacterial strain[7,69,70], though a reduction in photosynthetic activity is only observed in the last two situations[71]. We found at least one network with photosynthesis-related coding genes suppressed by ETI and not by PTI that could contribute to the differences observed in the status of chloroplast physiology between these immune responses.

Control of the abundance of membrane-localized of FLS2 receptor is key for modulating the perception of flg22. Several components of this control system have been identified[72–74], including degradation of FLS2 through selective autophagy, mediated by ATG8 and orosomucoid proteins[75]. Recently, subunits EXO70B1/2 of exocyst complex have been shown to modulate trafficking of FLS2 to the plasma membrane and PEN1 may independently participate in this process[64]. We identified a PTI- and ETI-induced lncRNA whose NCGs included PEN1. It is possible that this lncRNA modulates the abundance of PEN1 transcript and consequently affects the levels of FLS2 at the plasma membrane. This up-regulation of a typically PTI-associated gene upon PTI and ETI induction is consistent with fairly recent findings that indicate there is a crosstalk between these two responses[76,77].

Members of the GST protein family have been found to be transcriptionally induced upon PTI and ETI activation and contribute to mitigating oxidative stress[67]. We identified a set of 6 GSTs encoded in chromosome 9 of tomato, induced by PTI and/or ETI, that could potentially be transcriptionally regulated by MSTRG.16534.1. Tomato glutarredoxin *SlGRX*, which also contributes to preventing oxidative damage and promote resistance to *Phytophthora infestans*, can be induced by the neighboring lncRNA16397[48]. Further exploration of MSTRG.16534.1 network may shed light on a similar lncRNA-based control of oxidative damage.

To our knowledge our work represents the first report on tomato lncRNAs' participation against a bacterial pathogen, such as *Pst*. We believe the generated information will contribute to finding key regulatory modules controlling important processes during plant-pathogen interactions.

Methods

Tomato leaf transcript prediction and quantification. Raw RNA-seq reads from 33 samples of tomato leaves challenged with flg22, flgII-28 or different *Pseudomonas* spp. strains detailed in Table S1 were retrieved from Sequence Read Archive (SRA; https://www.ncbi.nlm.nih.gov/sra) available at NCBI. The complete set used accounted for 475 M reads (~ 21 Gb; 25×, 828 Mb genome). Reads were aligned to tomato rRNA sequences retrieved from SILVA database[78] using Bowtie[79] (v1.2.2) with the option-v 3 to allow a thorough removal of rRNA contamination. Clean reads were mapped to the tomato genome (assembly 3.00)[80] with Hisat2 program[81] (v2.1.0). Transcript assemblies and quantification were performed using Stringtie[81] (v1.3.3). Each alignment file was used to generate individual transcript assemblies, with the default setting of minimal transcript length of 200 bp, that were then merged into a single assembly by setting the option –merge. This merged assembly was used to estimate transcript abundance for each sample. Cuffcompare[82] (v2.2.1) along with tomato gene models (ITAG3.2)[80] allowed classifying 21,771 novel transcripts in class codes based on their relationship to annotated transcripts in the following categories of interest: *j*, potentially novel isoform (at least one splice junc-

tion shared with reference transcript); *i*, transcript falling entirely within a reference intron; *o*, generic exonic overlap with a reference transcript; *u*, unknown, intergenic transcript; *x*, exonic overlap with reference transcript on the opposite strand[59]. Differentially expressed transcripts were identified with DESeq2 software[83] (v1.26.0) using raw count data.

LncRNA identification and global characterization. Novel transcripts falling in the categories mentioned above were used as input for getorf stand-alone tool from EMBOSS (v6.6.0.0) which allowed the identification of 4,397 that had no open reading frame larger than 300 nt. From these, 2,677 had no homology to any peptide present in Pfam database (v31.0)[84] using blastx (Expect-value > 1e − 3). We employed CPC2 tool[85] to identify 2,668 transcripts with low coding potential. Finally to further remove transcripts that would not qualify as lncRNAs, we used batch sequence search tool from Rfam database[86] to filter other types of genomic and plastidial RNAs. After this stringent pipeline we kept 2,609 transcripts as putative tomato lncRNAs.

We used local blastn (-evalue 1e − 10 -soft_masking 'false' -num_alignments 1) to compare our predicted lncRNA with those available from previous works in tomato: leaves challenged with *Tomato yellow curl leaf virus* (TYCLV)[45,46,54] or *Phytophthora infestans*[48,55]; fruit pericarp tissue, roots infected with *Meloidogyne incognita* and leaves inoculated with *Potato spindle tuber viroid* from CANTATA database[56]; and four predicted tomato *TRANS-ACTING SIRNA3* (*TAS3*) transcripts[57].

To generate a graphical representation of the genomic distribution of protein-coding and lncRNAs we used software package Circos[87] (v0.69-8).

Neighboring co-regulated genes' identification, network generation and GO term analysis. Considering lncRNAs may modulate the expression of genes within a 100 kb up/down-stream region we identified their corresponding neighboring coding genes region[48,61–63]. Then for each DEL found in the comparisons mock_flgII-28_6h vs flgII-28_6h (PTI-flgII-28) and DC3000 Δ*fliC*Δ*avrPto*Δ*avrPtoB* vs DC3000 Δ*fliC* at 6 h in PtoR plants (ETI-AvrPto/AvrPtoB) we identified those neighboring protein-coding co-regulated genes (NCG), defined as having the same or opposite trend (|log2 fold-change| ≥ 1, q-value < 0.05). This information was used to generate NCG networks with Cytoscape program[88] (v3.8.2). We subjected the lists of NCGs identified for PTI-flgII-28 and ETI-AvrPto/AvrPtoB comparisons, to a GO term analysis using AgriGO v2.0[89] with default settings, ITAG3.2 as background and Plant GO Slim as gene ontology type. We analyzed separately those NCGs positively and negatively co-regulated in each comparison.

Clustering analysis. Given that the RNA-seq data used in this work derives from two separate experiments using different Rio Grande tomato backgrounds (RG-PtoR and RG-*prf3*, see Table S1), we performed two independent clustering analyses for each of them with Heatmapper online tool[90], using average linkage (clustering method) and Spearman rank correlation (distance measurement method). Input data in both cases were FPKM values of those expressed lncRNA (≥ 3 FPKM in at least one condition) with at least one q-value < 0.05 in any of the comparisons of interest.

Bacterial challenge and RT-qPCR assay. Four-week old Rio Grande PtoR (RG-PtoR) tomato plants, kindly provided by Prof. Gregory B. Martin, were syringe infiltrated on leaflets of their third true leaves, with mock solution (10 mM $MgCl_2$) or the following suspensions: 10^8 colony forming units (cfu)/mL of *Pseudomonas fluorescens* 55 (Pf 55), 5×10^6 cfu/mL *Pst* DC3000 (DC3000) and 5×10^6 cfu/mL *Pst* DC3000 Δ*avrPto*Δ*avrPtoB* (DC3000 ΔΔ). Mock vs Pf 55 accounts for PTI induction, while DC3000 ΔΔ vs DC3000 for AvrPto/AvrPtoB ETI induction. Six hours post infiltration (hpi) leaf tissue was frozen with N_2(l) and stored at -80 °C until use. Total RNA isolation and cDNA synthesis were performed as described previously[91]. RT-qPCR reaction mix consisted of: 5 µL of 2× SYBR Green/ROX Master Mix (PB-L, Bio-Logic Products), 2 µL of 2 µM primer mix, 0.2 µL of 50× ROX, 2 µL of a diluted 1:10 cDNA and miliQ H_2O to complete 10 µL final volume. Cycling conditions were 94 °C for 5 min and 45 cycles of 92 °C for 15 s, 60 °C for 20 s and 72 °C for 15 s. For gene expression analysis we selected one PTI/ETI-induced (MSTRG.17205.1), two PTI-induced (MSTRG.2922.1 and MSTRG.16686.1) and two ETI-induced (MSTRG.7999.1 and MSTRG.21751.1). Two reference genes (*ARD2* and *VIN3*) were used for normalization[53]. A list of primers used in this work can be found in Table S7. This study complied with local and national regulations.

Received: 3 September 2021; Accepted: 1 December 2021
Published online: 31 December 2021

References

1. Savary, S. *et al.* The global burden of pathogens and pests on major food crops. *Nat. Ecol. Evol.* **3**, 430–439. https://doi.org/10.1038/s41559-018-0793-y (2019).
2. Boutrot, F. & Zipfel, C. Function, discovery, and exploitation of plant pattern recognition receptors for broad-spectrum disease resistance. *Annu. Rev. Phytopathol.* **55**, 257–286. https://doi.org/10.1146/annurev-phyto-080614-120106 (2017).
3. Bentham, A. R. *et al.* A molecular roadmap to the plant immune system. *J. Biol. Chem.* **295**, 14916–14935. https://doi.org/10.1074/jbc.REV120.010852 (2020).
4. Schwessinger, B. & Ronald, P. C. Plant innate immunity: Perception of conserved microbial signatures. *Annu. Rev. Plant Biol.* **63**, 451–482. https://doi.org/10.1146/annurev-arplant-042811-105518 (2012).
5. Nguyen, H. P. *et al.* Methods to study PAMP-triggered immunity using tomato and *Nicotiana benthamiana*. *Mol. Plant Microbe Interact.* **23**, 991–999. https://doi.org/10.1094/MPMI-23-8-0991 (2010).

6. Monaghan, J. & Zipfel, C. Plant pattern recognition receptor complexes at the plasma membrane. *Curr. Opin. Plant Biol.* **15**, 349–357. https://doi.org/10.1016/j.pbi.2012.05.006 (2012).
7. Rosli, H. G. *et al.* Transcriptomics-based screen for genes induced by flagellin and repressed by pathogen effectors identifies a cell wall-associated kinase involved in plant immunity. *Genome Biol.* **14**, R139. https://doi.org/10.1186/gb-2013-14-12-r139 (2013).
8. Li, B., Meng, X., Shan, L. & He, P. Transcriptional regulation of pattern-triggered immunity in plants. *Cell Host Microbe* **19**, 641–650. https://doi.org/10.1016/j.chom.2016.04.011 (2016).
9. Macho, A. P. Subversion of plant cellular functions by bacterial type-III effectors: Beyond suppression of immunity. *New Phytol.* **210**, 51–57. https://doi.org/10.1111/nph.13605 (2016).
10. Toruno, T. Y., Stergiopoulos, I. & Coaker, G. Plant–pathogen effectors: Cellular probes interfering with plant defenses in spatial and temporal manners. *Annu. Rev. Phytopathol.* **54**, 419–441. https://doi.org/10.1146/annurev-phyto-080615-100204 (2016).
11. Moffett, P. Mechanisms of recognition in dominant R gene mediated resistance. *Adv. Virus Res.* **75**, 1–33. https://doi.org/10.1016/S0065-3527(09)07501-0 (2009).
12. Maekawa, T., Kufer, T. A. & Schulze-Lefert, P. NLR functions in plant and animal immune systems: So far and yet so close. *Nat. Immunol.* **12**, 817–826. https://doi.org/10.1038/ni.2083 (2011).
13. Tsuda, K., Sato, M., Stoddard, T., Glazebrook, J. & Katagiri, F. Network properties of robust immunity in plants. *PLoS Genet.* **5**, e1000772. https://doi.org/10.1371/journal.pgen.1000772 (2009).
14. Jones, J. D. & Dangl, J. L. The plant immune system. *Nature* **444**, 323–329 (2006).
15. Dodds, P. N. & Rathjen, J. P. Plant immunity: Towards an integrated view of plant-pathogen interactions. *Nat. Rev. Genet.* **11**, 539–548. https://doi.org/10.1038/nrg2812 (2010).
16. Wei, H. L., Zhang, W. & Collmer, A. Modular study of the type III effector repertoire in *Pseudomonas syringae* pv. *tomato* DC3000 reveals a matrix of effector interplay in pathogenesis. *Cell Rep.* **23**, 1630–1638. https://doi.org/10.1016/j.celrep.2018.04.037 (2018).
17. Pedley, K. F. & Martin, G. B. Molecular basis of Pto-mediated resistance to bacterial speck disease in tomato. *Annu. Rev. Phytopathol.* **41**, 215–243. https://doi.org/10.1146/annurev.phyto.41.121602.143032 (2003).
18. Oh, C. S. & Martin, G. B. Effector-triggered immunity mediated by the Pto kinase. *Trends Plant Sci.* **16**, 132–140. https://doi.org/10.1016/j.tplants.2010.11.001 (2011).
19. Gomez-Gomez, L. & Boller, T. FLS2: An LRR receptor-like kinase involved in the perception of the bacterial elicitor flagellin in Arabidopsis. *Mol. Cell* **5**, 1003–1011 (2000).
20. Chinchilla, D., Bauer, Z., Regenass, M., Boller, T. & Felix, G. The Arabidopsis receptor kinase FLS2 binds flg22 and determines the specificity of flagellin perception. *Plant Cell* **18**, 465–476 (2006).
21. Hind, S. R. *et al.* Tomato receptor FLAGELLIN-SENSING 3 binds flgII-28 and activates the plant immune system. *Nat. Plants* **2**, 16128. https://doi.org/10.1038/nplants.2016.128 (2016).
22. Xin, X. F. & He, S. Y. Pseudomonas syringae pv tomato DC3000: A model pathogen for probing disease susceptibility and hormone signaling in plants. *Annu. Rev. Phytopathol.* **51**, 473–498. https://doi.org/10.1146/annurev-phyto-082712-102321 (2013).
23. Cunnac, S. *et al.* Genetic disassembly and combinatorial reassembly identify a minimal functional repertoire of type III effectors in *Pseudomonas syringae*. *Proc Natl Acad Sci USA* **108**, 2975–2980. https://doi.org/10.1073/pnas.1013031108 (2011).
24. Martin, G. B. *et al.* Map-based cloning of a protein kinase gene conferring disease resistance in tomato. *Science* **262**, 1432–1436 (1993).
25. Tang, X. *et al.* Initiation of plant disease resistance by physical interaction of AvrPto and Pto kinase. *Science* **274**, 2060–2063 (1996).
26. Kraus, C. M., Munkvold, K. R. & Martin, G. B. Natural variation in tomato reveals differences in the recognition of AvrPto and AvrPtoB effectors from *Pseudomonas syringae*. *Mol. Plant.* **9**, 639–649. https://doi.org/10.1016/j.molp.2016.03.001 (2016).
27. Kung, J. T. Y., Colognori, D. & Lee, J. T. Long noncoding RNAs: Past, present, and future. *Genetics* **193**, 651–669. https://doi.org/10.1534/genetics.112.146704 (2013).
28. Long, Y., Wang, X., Youmans, D. T. & Cech, T. R. How do lncRNAs regulate transcription?. *Sci. Adv.* https://doi.org/10.1126/sciadv.aao2110 (2017).
29. Ma, L., Bajic, V. B. & Zhang, Z. On the classification of long non-coding RNAs. *RNA Biol.* **10**, 925–933. https://doi.org/10.4161/rna.24604 (2013).
30. Wang, K. C. & Chang, H. Y. Molecular mechanisms of long noncoding RNAs. *Mol. Cell* **43**, 904–914. https://doi.org/10.1016/j.molcel.2011.08.018 (2011).
31. Wu, L., Liu, S., Qi, H., Cai, H. & Xu, M. Research progress on plant long non-coding RNA. *Plants* https://doi.org/10.3390/plants9040408 (2020).
32. Karlik, E., Ari, S. & Gozukirmizi, N. LncRNAs: Genetic and epigenetic effects in plants. *Biotechnol. Biotechnol. Equip.* **33**, 429–439. https://doi.org/10.1080/13102818.2019.1581085 (2019).
33. Lucero, L., Fonouni-Farde, C., Crespi, M. & Ariel, F. Long noncoding RNAs shape transcription in plants. *Transcription* **11**, 160–171. https://doi.org/10.1080/21541264.2020.1764312 (2020).
34. Chekanova, J. A. Long non-coding RNAs and their functions in plants. *Curr. Opin. Plant Biol.* **27**, 207–216. https://doi.org/10.1016/j.pbi.2015.08.003 (2015).
35. Shafiq, S., Li, J. & Sun, Q. Functions of plants long non-coding RNAs. *Biochim. Biophys. Acta Gene Regul. Mech.* **155–162**, 2016. https://doi.org/10.1016/j.bbagrm.2015.06.009 (1859).
36. Bazin, J. *et al.* Global analysis of ribosome-associated noncoding RNAs unveils new modes of translational regulation. *Proc. Natl. Acad. Sci. USA* **114**, E10018. https://doi.org/10.1073/pnas.1708433114 (2017).
37. Zhang, Y.-C. *et al.* Genome-wide screening and functional analysis identify a large number of long noncoding RNAs involved in the sexual reproduction of rice. *Genome Biol.* **15**, 512. https://doi.org/10.1186/s13059-014-0512-1 (2014).
38. Csorba, T., Questa, J. I., Sun, Q. & Dean, C. Antisense *COOLAIR* mediates the coordinated switching of chromatin states at *FLC* during vernalization. *Proc. Natl. Acad. Sci. USA* **111**, 16160. https://doi.org/10.1073/pnas.1419030111 (2014).
39. Heo, J. B. & Sung, S. Vernalization-mediated epigenetic silencing by a long intronic noncoding RNA. *Science* **331**, 76. https://doi.org/10.1126/science.1197349 (2011).
40. Yuan, J. *et al.* Stress-responsive regulation of long non-coding RNA polyadenylation in *Oryza sativa*. *Plant J.* **93**, 814–827. https://doi.org/10.1111/tpj.13804 (2018).
41. Liu, J. *et al.* Genome-wide analysis uncovers regulation of long intergenic noncoding RNAs in *Arabidopsis*. *Plant Cell* **24**, 4333. https://doi.org/10.1105/tpc.112.102855 (2012).
42. Seo, J. S. *et al.* ELF18-induced long-noncoding RNA associates with mediator to enhance expression of innate immune response genes in Arabidopsis. *Plant Cell* **29**, 1024–1038. https://doi.org/10.1105/tpc.16.00886 (2017).
43. Wang, M., Zhao, W., Gao, L. & Zhao, L. Genome-wide profiling of long non-coding RNAs from tomato and a comparison with mRNAs associated with the regulation of fruit ripening. *BMC Plant Biol.* **18**, 75. https://doi.org/10.1186/s12870-018-1300-y (2018).
44. Zhu, B. *et al.* RNA sequencing and functional analysis implicate the regulatory role of long non-coding RNAs in tomato fruit ripening. *J. Exp. Bot.* **66**, 4483–4495. https://doi.org/10.1093/jxb/erv203 (2015).
45. Wang, J. *et al.* Genome-wide analysis of tomato long non-coding RNAs and identification as endogenous target mimic for microRNA in response to TYLCV infection. *Sci. Rep.* **5**, 16946. https://doi.org/10.1038/srep16946 (2015).
46. Zhou, Y. *et al.* Genome-wide identification of long non-coding RNAs in tomato plants irradiated by neutrons followed by infection with Tomato yellow leaf curl virus. *PeerJ* **7**, e6286. https://doi.org/10.7717/peerj.6286 (2019).

47. Zheng, Y., Wang, Y., Ding, B. & Fei, Z. Comprehensive transcriptome analyses reveal that potato spindle tuber viroid triggers genome-wide changes in alternative splicing, inducible trans-acting activity of phased secondary small interfering RNAs, and immune responses. *J. Virol.* https://doi.org/10.1128/JVI.00247-17 (2017).
48. Cui, J., Luan, Y., Jiang, N., Bao, H. & Meng, J. Comparative transcriptome analysis between resistant and susceptible tomato allows the identification of lncRNA16397 conferring resistance to *Phytophthora infestans* by co-expressing glutaredoxin. *Plant J.* **89**, 577–589. https://doi.org/10.1111/tpj.13408 (2017).
49. Cui, J. *et al.* Genome-wide identification of LncRNAs and analysis of CeRNA networks during tomato resistance to *Phytophthora infestans*. *Phytopathology* https://doi.org/10.1094/PHYTO-04-19-0137-R (2019).
50. Hou, X. *et al.* LncRNA39026 enhances tomato resistance to *Phytophthora infestans* by decoying miR168a and inducing PR gene expression. *Phytopathology* **110**, 873–880. https://doi.org/10.1094/PHYTO-12-19-0445-R (2020).
51. Jiang, N. *et al.* Sly-lncRNA15492 interacts with Sly-miR482a and affects *Solanum lycopersicum* immunity against *Phytophthora infestans*. *Plant J.* https://doi.org/10.1111/tpj.14847 (2020).
52. Pombo, M. A. *et al.* Transcriptomic analysis reveals tomato genes whose expression is induced specifically during effector-triggered immunity and identifies the Epk1 protein kinase which is required for the host response to three bacterial effector proteins. *Genome Biol.* **15**, R492. https://doi.org/10.1186/s13059-014-0492-1 (2014).
53. Pombo, M. A., Zheng, Y., Fei, Z., Martin, G. B. & Rosli, H. G. Use of RNA-seq data to identify and validate RT-qPCR reference genes for studying the tomato-*Pseudomonas* pathosystem. *Sci. Rep.* **7**, 44905. https://doi.org/10.1038/srep44905 (2017).
54. Wang, J. *et al.* Re-analysis of long non-coding RNAs and prediction of circRNAs reveal their novel roles in susceptible tomato following TYLCV infection. *BMC Plant Biol.* **18**, 104. https://doi.org/10.1186/s12870-018-1332-3 (2018).
55. Cui, J. *et al.* LncRNA33732-respiratory burst oxidase module associated with WRKY1 in tomato-*Phytophthora infestans* interactions. *Plant J.* https://doi.org/10.1111/tpj.14173 (2018).
56. Szcześniak, M. W., Rosikiewicz, W. & Makałowska, I. CANTATAdb: A collection of plant long non-coding RNAs. *Plant Cell Physiol.* https://doi.org/10.1093/pcp/pcv201 (2016).
57. Xia, R., Xu, J. & Meyers, B. C. The emergence, evolution, and diversification of the miR390-TAS3-ARF pathway in land plants. *Plant Cell* **29**, 1232–1247. https://doi.org/10.1105/tpc.17.00185 (2017).
58. Altschul, S. F. *et al.* Gapped BLAST and PSI-BLAST: A new generation of protein database search programs. *Nucleic Acids Res.* **25**, 3389–3402 (1997).
59. Pertea, G. & Pertea, M. GFF utilities: GffRead and GffCompare. *F1000Res* **9**, ISCB Comm J-304 (2020).
60. Zhang, N., Pombo, M. A., Rosli, H. G. & Martin, G. B. Tomato wall-associated kinase SlWak1 depends on Fls2/Fls3 to promote apoplastic immune responses to *Pseudomonas syringae*. *Plant Physiol.* https://doi.org/10.1104/pp.20.00144 (2020).
61. Liao, Q. *et al.* Large-scale prediction of long non-coding RNA functions in a coding–non-coding gene co-expression network. *Nucleic Acids Res.* **39**, 3864–3878. https://doi.org/10.1093/nar/gkq1348 (2011).
62. Huang, X. *et al.* Genome-wide identification and characterization of long non-coding RNAs involved in flag leaf senescence of rice. *Plant Mol. Biol.* **105**, 655–684. https://doi.org/10.1007/s11103-021-01121-3 (2021).
63. Tian, Y. *et al.* Genome-wide identification and characterization of long non-coding RNAs involved in fruit ripening and the climacteric in *Cucumis melo*. *BMC Plant Biol.* **19**, 369. https://doi.org/10.1186/s12870-019-1942-4 (2019).
64. Wang, W. *et al.* The *Arabidopsis* exocyst subunits EXO70B1 and EXO70B2 regulate FLS2 homeostasis at the plasma membrane. *New Phytol.* **227**, 529–544. https://doi.org/10.1111/nph.16515 (2020).
65. Varet, A., Hause, B., Hause, G., Scheel, D. & Lee, J. The Arabidopsis NHL3 gene encodes a plasma membrane protein and its overexpression correlates with increased resistance to *Pseudomonas syringae* pv. *tomato* DC3000. *Plant Physiol.* **132**, 2023–2033. https://doi.org/10.1104/pp.103.020438 (2003).
66. Okuda, K., Myouga, F., Motohashi, R., Shinozaki, K. & Shikanai, T. Conserved domain structure of pentatricopeptide repeat proteins involved in chloroplast RNA editing. *Proc. Natl. Acad. Sci. USA* **104**, 8178–8183. https://doi.org/10.1073/pnas.0700865104 (2007).
67. Gullner, G., Komives, T., Király, L. & Schröder, P. Glutathione S-transferase enzymes in plant–pathogen interactions. *Front. Plant Sci.* **9**, 1836 (2018).
68. Martin, G. B. Suppression and activation of the plant immune system by *Pseudomonas syringae* effectors AvrPto and AvrPtoB. in *Effectors in Plant–Microbe Interactions* (eds F. Martin & S. Kamoun) 123–154 (Wiley-Blackwell, 2011).
69. Truman, W., de Zabala, M. T. & Grant, M. Type III effectors orchestrate a complex interplay between transcriptional networks to modify basal defence responses during pathogenesis and resistance. *Plant J.* **46**, 14–33. https://doi.org/10.1111/j.1365-313X.2006.02672.x (2006).
70. de Torres Zabala, M. *et al.* Chloroplasts play a central role in plant defence and are targeted by pathogen effectors. *Nat. Plants* **1**, 15074. https://doi.org/10.1038/nplants.2015.74 (2015).
71. Littlejohn, G.A.-O., Breen, S.A.-O., Smirnoff, N.A.-O. & Grant, M.A.-O. Chloroplast immunity illuminated. *New Phytol* **229**, 3038–3107. https://doi.org/10.1111/nph.17076 (2021).
72. Lee, H. Y. *et al.* Arabidopsis RTNLB1 and RTNLB2 reticulon-like proteins regulate intracellular trafficking and activity of the FLS2 immune receptor. *Plant Cell* **23**, 3374–3391. https://doi.org/10.1105/tpc.111.089656 (2011).
73. Choi, S.-W. *et al.* RABA members act in distinct steps of subcellular trafficking of the FLAGELLIN SENSING2 receptor. *Plant Cell* **25**, 1174–1187. https://doi.org/10.1105/tpc.112.108803 (2013).
74. Shen, Q., Bourdais, G., Pan, H., Robatzek, S. & Tang, D. *Arabidopsis* glycosylphosphatidylinositol-anchored protein LLG1 associates with and modulates FLS2 to regulate innate immunity. *Proc. Natl. Acad. Sci. USA* **114**, 5749. https://doi.org/10.1073/pnas.1614468114 (2017).
75. Yang, F. *et al.* A plant immune receptor degraded by selective autophagy. *Mol. Plant* **12**, 113–123. https://doi.org/10.1016/j.molp.2018.11.011 (2019).
76. Ngou, B. P. M., Ahn, H.-K., Ding, P. & Jones, J. D. G. Mutual potentiation of plant immunity by cell-surface and intracellular receptors. *Nature* **592**, 110–115. https://doi.org/10.1038/s41586-021-03315-7 (2021).
77. Yuan, M., Ngou, B. P. M., Ding, P. & Xin, X.-F. PTI-ETI crosstalk: An integrative view of plant immunity. *Curr. Opin. Plant Biol.* **62**, 102030. https://doi.org/10.1016/j.pbi.2021.102030 (2021).
78. Quast, C. *et al.* The SILVA ribosomal RNA gene database project: Improved data processing and web-based tools. *Nucleic Acids Res.* **41**, D590-596. https://doi.org/10.1093/nar/gks1219 (2013).
79. Langmead, B., Trapnell, C., Pop, M. & Salzberg, S. L. Ultrafast and memory-efficient alignment of short DNA sequences to the human genome. *Genome Biol.* **10**, R25. https://doi.org/10.1186/gb-2009-10-3-r25 (2009).
80. Fernandez-Pozo, N. *et al.* The Sol Genomics Network (SGN)–from genotype to phenotype to breeding. *Nucleic Acids Res.* **43**, D1036-1041. https://doi.org/10.1093/nar/gku1195 (2015).
81. Pertea, M., Kim, D., Pertea, G. M., Leek, J. T. & Salzberg, S. L. Transcript-level expression analysis of RNA-seq experiments with HISAT, StringTie and Ballgown. *Nat. Protoc.* **11**, 1650–1667. https://doi.org/10.1038/nprot.2016.095 (2016).
82. Trapnell, C. *et al.* Transcript assembly and quantification by RNA-Seq reveals unannotated transcripts and isoform switching during cell differentiation. *Nat. Biotechnol.* **28**, 511–515. https://doi.org/10.1038/nbt.1621 (2010).
83. Love, M. I., Huber, W. & Anders, S. Moderated estimation of fold change and dispersion for RNA-seq data with DESeq2. *Genome Biol.* **15**, 1–21. https://doi.org/10.1186/s13059-014-0550-8 (2014).

84. El-Gebali, S. *et al.* The Pfam protein families database in 2019. *Nucleic Acids Res.* **47**, D427–D432. https://doi.org/10.1093/nar/gky995 (2019).
85. Kang, Y.-J. *et al.* CPC2: A fast and accurate coding potential calculator based on sequence intrinsic features. *Nucleic Acids Res.* **45**, W12–W16. https://doi.org/10.1093/nar/gkx428 (2017).
86. Kalvari, I. *et al.* Rfam 13.0: Shifting to a genome-centric resource for non-coding RNA families. *Nucleic Acids Res.* **46**, D335–D342. https://doi.org/10.1093/nar/gkx1038 (2018).
87. Krzywinski, M. I. *et al.* Circos: An information aesthetic for comparative genomics. *Genome Res.* https://doi.org/10.1101/gr.092759.109 (2009).
88. Shannon, P. *et al.* Cytoscape: A software environment for integrated models of biomolecular interaction networks. *Genome Res.* **13**, 2498–2504. https://doi.org/10.1101/gr.1239303 (2003).
89. Tian, T. *et al.* agriGO v2.0: A GO analysis toolkit for the agricultural community, 2017 update. *Nucleic Acids Res.* **45**, W122–W129. https://doi.org/10.1093/nar/gkx382 (2017).
90. Babicki, S. *et al.* Heatmapper: Web-enabled heat mapping for all. *Nucleic Acids Res.* **44**, W147–W153. https://doi.org/10.1093/nar/gkw419 (2016).
91. Ramos, R. N., Martin, G. B., Pombo, M. A. & Rosli, H. G. WRKY22 and WRKY25 transcription factors are positive regulators of defense responses in *Nicotiana benthamiana*. *Plant Mol. Biol.* https://doi.org/10.1007/s11103-020-01069-w (2021).

Acknowledgements

We thank Prof. Aureliano Bombarely (Università degli Studi di Milano, Italy) for kindly providing access to a high performance server used for bioinformatic analyses, Dr. Diana Lauff for technical assistance and Mauro Bartolozzi and Santiago Martínez Alonso for plant care. This research was supported by Agencia Nacional de Promoción Científica y Técnica—Argentina (PICT 2017-0916 and PICT 2019-1328) and Consejo Nacional de Investigaciones Científicas y Técnicas—Argentina (PUE-INFIVE 2016-0110 and PIO UNLP-CONICET 2017).

Author contributions

H.G.R. and M.A.P. designed the research; H.G.R., E.S., F.N.B., R.N.R. and M.A.P., performed the research; H.G.R., E.S. and M.A.P., analyzed the data; H.G.R. and M.A.P. wrote the manuscript. All authors read and approved the manuscript.

Competing interests

The authors declare no competing interests.

Additional information

Supplementary Information The online version contains supplementary material available at https://doi.org/10.1038/s41598-021-04005-0.

Correspondence and requests for materials should be addressed to H.G.R. or M.A.P.

Reprints and permissions information is available at www.nature.com/reprints.

Publisher's note Springer Nature remains neutral with regard to jurisdictional claims in published maps and institutional affiliations.